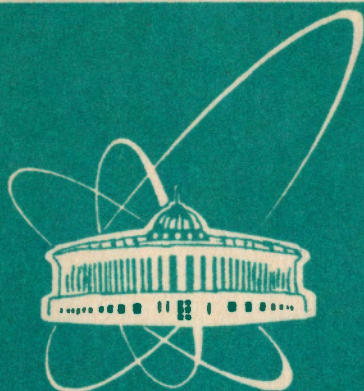


93-68



СООБЩЕНИЯ
ОБЪЕДИНЕННОГО
ИНСТИТУТА
ЯДЕРНЫХ
ИССЛЕДОВАНИЙ
ДУБНА

E9-93-68

D.I.Kaltchev, E.A.Perelstein

SYNCHROTRON RADIATION CALCULATIONS
AND COLLIMATOR DESIGN
FOR THE TAU-CHARM FACTORY

1993

I. INTRODUCTION

Design study of the high luminosity symmetric e^+e^- collider in Dubna (Tau-Charm factory) was published in /1,2/. The main accelerator parameters are: energy 2.2 GeV, total current $J=0.6$ A, horizontal emittance $\epsilon_x = 4.1 \cdot 10^{-7}$ m, vertical emittance $\epsilon_y = 2 \cdot 10^{-8}$ m.

An important constraint on the design is the background expected from synchrotron radiation (SR) /3-6/. A care must to be taken in minimizing the SR via the layout of the magnet system.

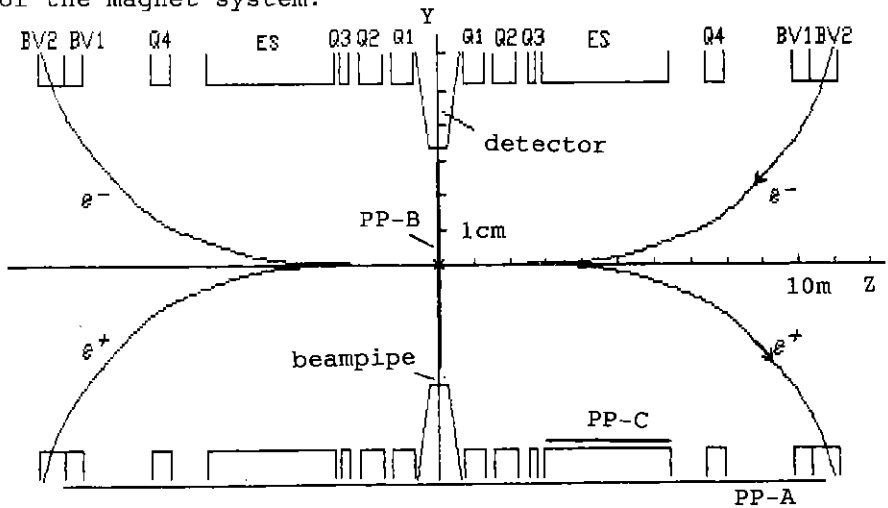


Fig.1 Layout of the magnetic elements in the interaction region (IR) of the Tau-Charm factory. Several positions of the SYNRAD projection plane are shown: PP-A, PP-B, PP-C.

SR is produced when an electron or positron is bent in the magnetic field of a dipole or quadrupole. The magnetic lattice in the IR is shown on Fig.1 - the e^+ and e^- beams are separated symmetrically by the use of the electrostatic separator ES, the offset quadrupole Q4 and the bending magnets BV1 and BV2. Minimal beam dimensions at the

interaction point (IP) are achieved by means of the low β S.C. quadrupoles Q1, Q2, Q3.

The thin beampipe (Fig.1) made from beryllium and lined with a thin layer of Cu is centered around the IP and separates the detector and accelerator volumes. To protect the beampipe from direct SR some masks must be foreseen on either side of the IP. Most of the SR photons pass through the IR without interaction or are adsorbed in the masks and in the chamber walls. Due to Compton scattering and induce fluorescence some secondary photons appear, which may pass through the beam pipe and enter the detector.

The acceptable level of backgrounds are is defined by the following criteria /3,4,6/: the maximal dose which the detector can stand without being damaged, the maximal occupancy, i.e. the highest tolerable probability of background hits and the maximum heat load for which adequate cooling of the beampipe can be supplied. Because of its proximity to the IP, silicon vertex detector is most subject to radiation damage. For a minimum lifetime of 10^7 s the energy deposition per time and area in 200 μm thick silicon layer must not exceed 10^{-9} W/cm². For the central track chambers an occupancy of several percent is considered the limit of for proper performance.

II. SR SIMULATION PROGRAM

We present a fast algorithm for determination the SR intensity incident on the surfaces of interest (e.g. the vacuum chamber walls, the beampipe, the mask sides, the ES electrodes). The program SYNRAD works in interactive regime displaying the topology of the SR spots on these surfaces. The maximum calculation time needed (for integration over the total photon energy interval) is less than 10 min. SYNRAD uses many of the ideas already suggested in similar SR-modeling programs /3,4/.

SYNRAD works in the following way. First, an

appropriate plane is defined by the user - we refer to it below as projection plane (PP). No restrictions on the slope of PP or on its distance to the IP are assumed, but it must be perpendicular to the YZ-plane and must cross the SR fan (or fans). Secondly, the SR produced by the beam passing through one or several magnetic elements is projected on the projection plane and the distribution of power density (or number of photons/s) is compiled. Choosing the PP position so that it coincides or is tangential to the surfaces of interests we obtain picture of the SR propagation in the interaction region.

We choose rectangular coordinate systems:

- 1) beam coordinate system $(\vec{z}, \vec{x}, \vec{y})$ with origin in the current point s , the \vec{y} -axes lies in the central trajectory plane, the \vec{z} -axes is tangential to the central trajectory.
- 2) laboratory coordinate system $(\vec{X}, \vec{Y}, \vec{Z})$ with origin in the IP, the \vec{Y} -axes lies in the central trajectory plane.
- 3) transversal coordinates on the PP: (x_w, y_w) .

The program accepts as input:

- a machine lattice file produced by MAD, in which magnet positions, lengths and strengths are specified;
- the central beam trajectory $Y_c(s), Z_c(s)$ and the beta functions as calculated by MAD; s is the coordinate along the central beam trajectory;
- the beam energy (2.2 GeV) and the horizontal and vertical emittances;
- the projection plane position in space;
- the photon energy interval required.

At the program output we obtain distribution of the SR power density (or number of photons/s) on the projection plane. Some positions of the projection plane (PP-A, PP-B, PP-C) used in calculations are shown on Fig.1.

SYNRAD starts with calculating the central trajectory and the beam-stay-clear envelopes $\sigma_x(s)$ and $\sigma_y(s)$ with step 1 cm over the longitudinal coordinate s inside every

magnetic element (SPLINE method). A simplifying assumption in the beam model consist in neglecting the width of the phase space ellipse, thus assuming definite correlation between x and $x'=dx/ds$ and between y and $y'=dy/ds$ /3/. This makes it possible to define a 3D velocity field $\vec{v}(s,x,y)$. At each beam point s,x,y the direction of \vec{v} is defined by

$$\operatorname{tg}(\alpha_x) = (\sigma'_x / \sigma_x) x; \quad \operatorname{tg}(\alpha_y) = (\sigma'_y / \sigma_y) y. \quad (1)$$

where α_x, α_y are angles between z -axes and the projections of the vector \vec{v} on the (\vec{x}, \vec{z}) и (\vec{y}, \vec{z}) planes. The radiation of a pointlike SR source located at X_s, Y_s, Z_s is propagating along the line

$$\begin{aligned} Y &= (Z - Z_s) \operatorname{tg}(\alpha_c + \alpha_y + \epsilon) + Y_s, \\ X &= (Z - Z_s) \operatorname{tg}(\alpha_c + \alpha_x) + X_s, \\ \epsilon &= \pm 1 / (2\gamma); \end{aligned} \quad (2)$$

α_c is the angular offset (for fixed s) of the central trajectory: $\operatorname{tg}(\alpha_c) = dY_c / dZ_c$. The parameter ϵ appears because of the angular spread of the SR in the \vec{y}, \vec{z} plane (see below).

Point to point transformation

Let (x_w, y_w) are rectangular coordinates on the PP. For given s the coordinates x_w, y_w at which the line (2) intersects the PP can be expressed by the source coordinates x, y in terms of elementary functions, thus defining the transformation $(x, y) \rightarrow (x_w, y_w)$. However, the reverse transformation $(x_w, y_w) \rightarrow (x, y)$ can be analytically found only in case that $\epsilon = 0$.

Mapping

We first divide the PP into rectangular cells $dx_w dy_w$.

We divide the beam along its central trajectory into 1cm segments and each segment in both transverse dimensions x, y into current elements each having volume $dx dy ds$. The

elementary radiation fan (Fig.2) is formed by four lines of the kind (Eq.2) - the upper two with $\epsilon = -1/(2\gamma)$ and the lower two - with $\epsilon = 1/(2\gamma)$. In such a way the $1/\gamma$ angular spread of the radiation is taken into account only in vertical direction. The cross-section of the elementary fan with the PP is an appropriate quadrangle (Fig.2). We assume that the SR intensity radiated by the volume $dx dy ds$ is uniformly distributed over the quadrangle area, so this intensity should be distributed proportionally over the PP-cells $dx_w dy_w$ (each cell is given a portion proportional to its fraction of quadrangle's area). Finally we integrate 1) over the transverse beam coordinates x, y from -10σ to 10σ multiplying at each point x, y by the appropriate gaussian weight; 2) over the coordinate s from the beginning to the end of the magnet; 3) over the photon energy interval (only in case of quadrupole).

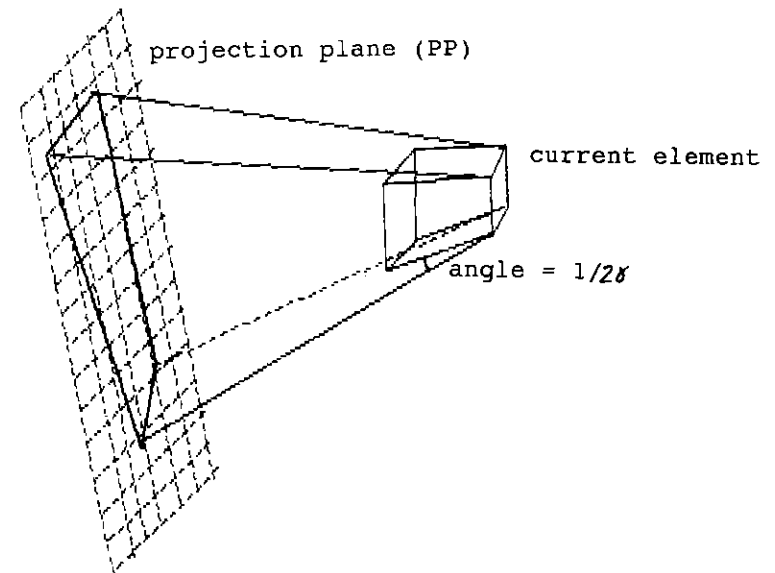


Fig.2 Mapping from a beam element $dx dy ds$ to the PP with taking into account the vertical $1/\gamma$ angle spread of the SR.

SYNRAD divides the machine magnetic elements into two groups and uses different procedures of mapping for each group:

1) "near" sources (to the IP) - quadrupoles Q1,Q2,Q3; the $1/\gamma$ angle spread of SR is neglected so $\varepsilon=0$ and the reverse transformation $(x_w, y_w) \rightarrow (x, y)$ is used. This sufficiently simplifies the calculations.

2) "distant" sources or bending magnets - ES, the offset quadrupole Q4, BV1 and BV2. The $1/\gamma$ angle spread of SR is taken into account.

When calculating the SR produced in the beam volume $dx dy ds$ we need to know the local radius of the electron trajectory. Inside the bending magnet (ES, Q4, BV1, BV2) it is assumed to be constant ($\rho = \text{const}$) for all x, y . Inside a quadrupole with strength k :

$$\rho(x, y) = k^{-1} (x^2 + y^2)^{-1/2}$$

To verify the SYNRAD results we use the following criteria:

1. The total intensity radiated by any magnetic element must not depend on the steps dx, dy, dz, dx_w, dy_w , or on the PP position in space. SYNRAD satisfies this with an accuracy better than 10^{-2} .

2. The total power radiated by the beam passing a quadrupole must not be far from

$$P_{\text{tot}} [\text{W}] = 7 \cdot 10^{-8} \gamma^4 J[\text{A}] K^2 (\bar{\sigma}_x^2 + \bar{\sigma}_y^2) l_{\text{elem}}, \quad (3)$$

where $\bar{\sigma}_{x, y} = \frac{1}{2} (\sigma_{x, y}^{\text{max}} + \sigma_{x, y}^{\text{min}})$,

$$\sigma_{x, y}^{\text{max}} = \max_S (\sigma_{x, y}(s)); \quad \sigma_{x, y}^{\text{min}} = \min_S (\sigma_{x, y}(s)),$$

$l_{\text{elem}} = s_{\text{fin}} - s_{\text{beg}}$ is the quadrupole length in cm.

3. The total power and number of photons/s radiated by the beam passing a bending magnet can be found exactly:

$$P_{\text{tot}} [\text{W}] = 8,57 \cdot 10^{-8} \gamma^4 J[\text{A}] \rho^{-2} [\text{cm}] l_{\text{elem}}; \quad (4)$$

$$\frac{dN}{dt} [\text{c}^{-1}] = 6,2 \cdot 10^{16} \gamma J[\text{A}] \frac{l_{\text{elem}}}{\rho [\text{cm}]}$$

III. RESULTS

"Distant" sources

The parameters of the "distant" sources are shown in Table 1. The total number of photons/s and the total power in Table 1 are calculated by Eq.4. SYNRAD obtains the same values with an accuracy 10^{-3} . This result does not depend on the position of PP.

Table 1. Parameters of the "distant" sources.

bend	length cm	ρ m	u_c eV	$dN/dt _{\text{tot}}$ s^{-1}	P_{tot} W
ES	340	10^3	23,6	$5,4 \cdot 10^{17}$	0,68
Q4	60	112,3	210	$8,5 \cdot 10^{17}$	9,4
BV1	50	59,5	397	$1,3 \cdot 10^{18}$	28
BV2	70	41,6	567	$2,7 \cdot 10^{18}$	80

"Near" sources

The quadrupole parameters are given in Table 2. Here the total number of photons/sec, the total power and the average critical energy u_c of the radiation are found by SYNRAD (u_c is defined as $u_c \approx 3u_{\text{max}}$, where u_{max} corresponds to the maximum of the spectrum. The corresponding values of P_{tot} calculated by Eqn.3 are shown in Table 3.

Table 2. Parameters of the "near" sources.

quadr.	length cm	k m ⁻²	u _c eV	dN/dt _{tot} s ⁻¹	P _{tot} W
Q1	50	-3.66	150	3.8 10 ¹⁷	6
Q2	50	3.55	300	4 10 ¹⁷	16
Q3	20	-3.51	180	1.1 10 ¹⁷	3

Table 3.

quadrupole	P _{tot} , W	Eqn.3
Q1	6	4.8
Q2	16	17.6
Q3	3	3.8

SR in the interaction region

Here we discuss the power and photons/sec levels on all surfaces within ±12m. We use the following positions of the Projection Plane (Fig.1):

PP-A: PP is tangential to the vacuum chamber wall (radius 6 cm);

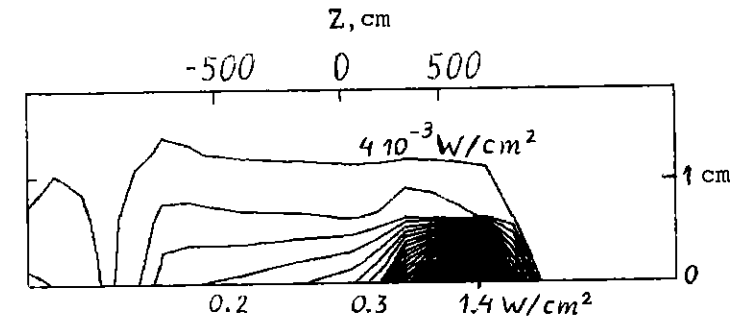
PP-B: PP is normal to the beams and passes the IP;

PP-C: PP coincides with the lower pair of separator electrodes (at radius 5cm).

Power density along the vacuum chamber wall (radius 6 cm, PP-A) is shown on Fig.3a. Fig.3b shows the topology of the corresponding SR spot, its maximal transverse size is roughly 1cm.

Fig.4 shows the distribution near the IP (PP-B) of photons having energies more than 1keV and produced inside the three quadrupoles Q1,Q2,Q3. This radiation passes through the detector region without striking any surfaces.

The electrostatic separator ES consists of two pairs of electrodes - upper and lower. Almost all the SR produced inside the magnet BV1 passes through the gap between the



б)

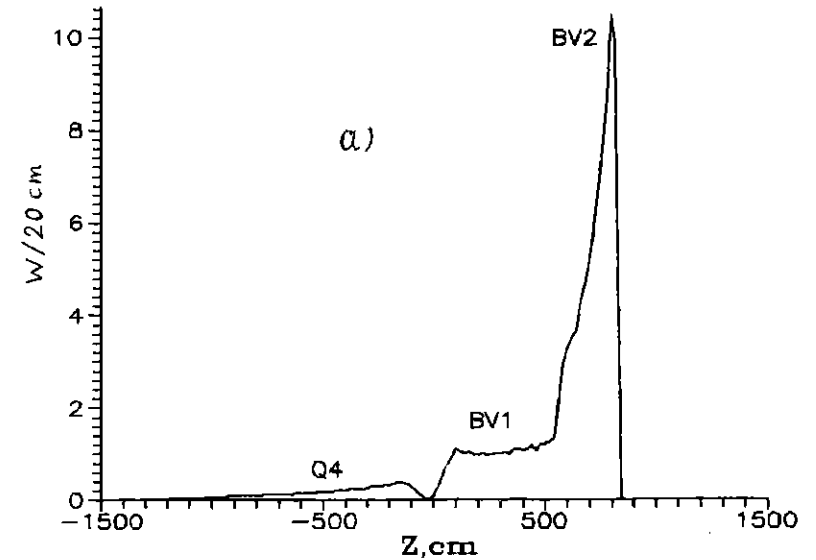


Fig. 3a Power density, deposited by one beam into the vacuum chamber wall (radius 6 cm):

- a) linear power distribution;
- б) a half of the SR spot.

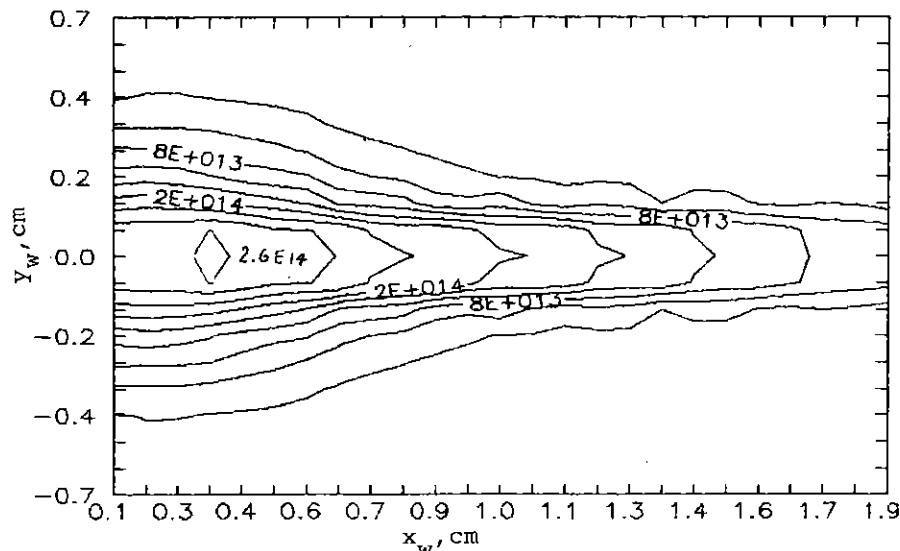


Fig.4 SR intensity incident on the PP-B in units number phot. > 1 keV/s/mm², produced by the set of low β quadrupoles Q1, Q2, Q3.

lower pair of electrodes. In the considered variant of magnetic system the magnet BV is divided into two parts (a weaker magnet BV1 and a stronger - BV2) in order to diminish SR striking the separator. The SR produced in the stronger magnet BV2 does not reach the separator. Using position PP-C of the projection plane we find that if the gap size is 2 cm then the power density incident on the ES electrode is less than $5 \cdot 10^{-3}$ W/cm².

SR backgrounds without masks

We take the following parameters for the thin portion of the beampipe: radius 3.5 cm, length 24 cm, materials 25 μ m Cu + 1mm Be.

Without masks 0.4 W/beam are incident on the beampipe surface corresponding to $3.2 \cdot 10^{16}$ phot./s/beam. This SR is produced in the quadrupole Q4. The SR fans from the other magnets pass through the IP without striking any surfaces

(Q1, Q2, Q3); pass through the narrow gap between the lower pair of ES-electrodes (BV1) or intercept the vacuum chamber wall near the separator (BV2).

The energy spectrum is quite soft as it can be seen in Table 4 (one beam).

Table 4. Energy spectrum of the photons striking the nonmasked beampipe

phot. energy interval	numb.phot./s
all (> 0keV)	$3.2 \cdot 10^{16}$
> 1keV	$3.5 \cdot 10^{13}$
> 2keV	$8.5 \cdot 10^{10}$
> 4keV	$4.3 \cdot 10^6$
> 6keV	300

The average power density incident on the beampipe surface is $7.7 \cdot 10^{-4}$ W/cm² ($6 \cdot 10^{13}$ phot./s/cm²). Taking $7 \cdot 10^{-7}$ for the transmission coefficient we obtain that $5.4 \cdot 10^{-10}$ W/cm² penetrate through the beampipe and are incident on the first layer of silicon. This nears the allowed limit (10^{-9}) so masking is necessary.

Masking

Here we consider two variants of masking to shield the beampipe against direct radiation. The geometries are shown on Fig.5 and Fig.6 and the corresponding statistics of photons with taking into account reflection of photons from the mask tips and from the mask surfaces are shown on Tables 5 and 6. The average angle between the direction of the Q4-radiation fan and the Z-axis is 7 mrad.

In Variant 1 (short symmetric masks) two equal tantalum masks are situated symmetrically on the both sides of IP. The side 1A of mask 1 doesn't have line-of-sight to the detector beampipe so the reflected photons can not directly reach the detector. To estimate the number of photons scattered from the tip of mask 1 (Table 1) we use

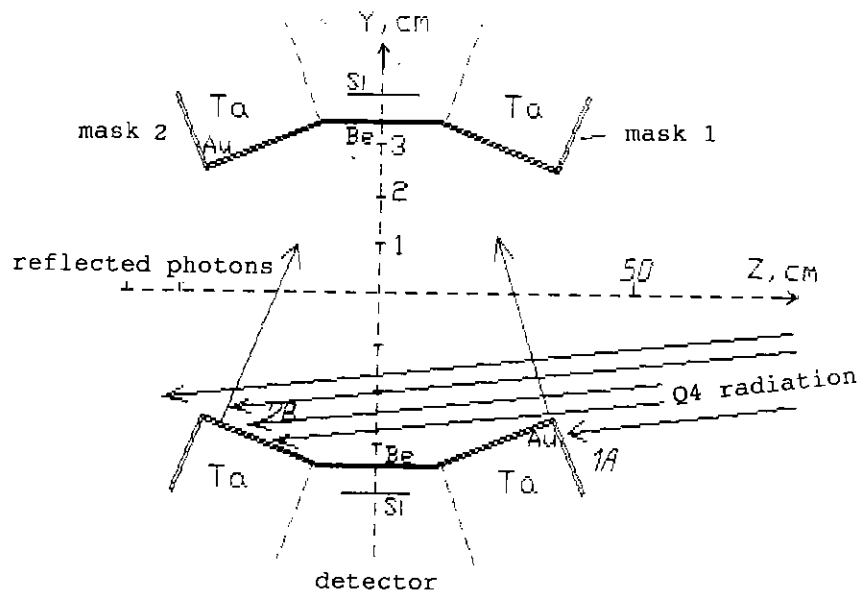


Fig.5 Variant 1 of masking (short symmetric masks). The angle between the 2B side of mask 2 and the Y-axis is 87.5° . Number of photons scattered from the mask-1 tip $= 2 \cdot 10^7$. Of them ~ 20 phot./s enter the detector. Main background source (10^6 phot./s) are the photons reflected from the side B2 ($1.4 \cdot 10^{12}$ phot./s).

the method proposed in /3/ - we assume that the corner of the mask has a $1 \mu\text{m}$ radius. The largest background source is backscattering of radiation from the side 2B. On this side Q4 deposits 1.3 W or $1.1 \cdot 10^{17}$ phot./s distributed along 12 cm length down from the mask tip. Multiplying to an averaged solid angle fraction (0.016) and to the reflecting coefficient for Ta ($8 \cdot 10^{-4}$) we obtain that $1.4 \cdot 10^{12}$ phot./s reflecting from the side 2B strike the beampipe surface. Of these 10^6 phot./s ($1.2 \cdot 10^3$ phot./s $> 1 \text{ keV/s}$) penetrate the beampipe and enter the detector. In order to decrease this source of backgrounds we increase the slope of 2B side which leads to asymmetric masks. These are considered in Variant 2.

	incident on the mask numb.phot/s s^{-1}	incident on the Be pipe numb.phot/s s^{-1}	enter the detector numb.phot/s s^{-1}
mask 1			
>0keV	$6.5 \cdot 10^{17}$	$2 \cdot 10^7$	20
>1keV	$7.1 \cdot 10^{14}$	$2.1 \cdot 10^4$	0
mask 2			
>0keV	$1 \cdot 10^{17}$	$1.4 \cdot 10^{12}$	10^6
>1keV	$1.3 \cdot 10^{14}$	$1.7 \cdot 10^9$	$1.2 \cdot 10^3$
total			
>0keV	$7.5 \cdot 10^{17}$	$1.4 \cdot 10^{12}$	10^6
>1keV	$8.4 \cdot 10^{14}$	$1.7 \cdot 10^9$	$1.2 \cdot 10^3$

Table 5. SR backgrounds (from 1 beam) for Variant 1.

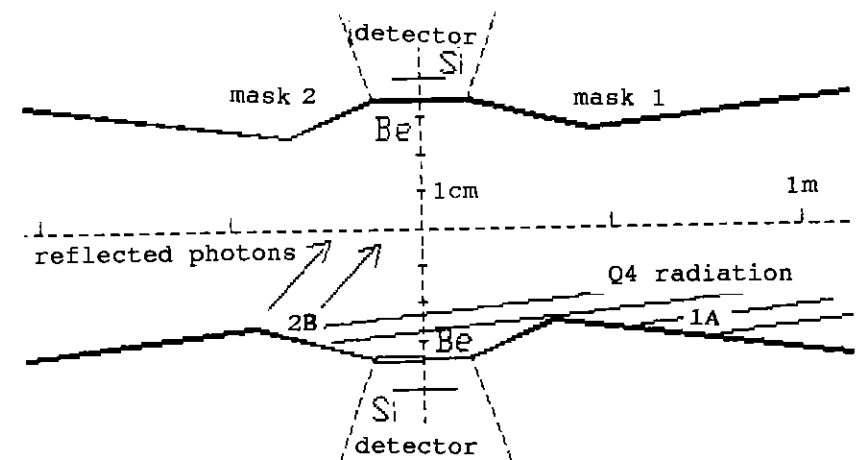


Fig.6 Variant 2 of masking (long asymmetric masks). The angle between the 2B side of mask 2 and the Y-axis is 88.5° . Photons reflected from side 1A ($1.4 \cdot 10^{11}$ phot./s) and from the side 2B ($6 \cdot 10^{11}$ phot./s) are incident on the Be surface. Of them $5.2 \cdot 10^5$ phot./s enter the detector.

In Variant 2 (long asymmetric masks) the length of the masks is increased. Although photons that scatter from side 1A have direct line-of-sight to the detector beampipe the final backgrounds are even less than in Variant 1. This is because the backscattering from side 2B here is much lower.

	incident on the mask numb.phot/s s^{-1}	incident on the Be pipe numb.phot/s s^{-1}	enter the detector numb.phot/s s^{-1}
mask 1			
>0keV	$6.5 \cdot 10^{17}$	$1.4 \cdot 10^{11}$	10^5
>1keV	$7.1 \cdot 10^{14}$	$1.6 \cdot 10^8$	110
>2keV	$3.8 \cdot 10^{12}$	$8 \cdot 10^5$	0
mask 2			
>0keV	$1.10 \cdot 10^{17}$	$6 \cdot 10^{11}$	$4.2 \cdot 10^5$
>1keV	$1.3 \cdot 10^{14}$	$7.6 \cdot 10^8$	530
>2keV	$8.2 \cdot 10^{11}$	$4 \cdot 10^6$	3
total			
>0keV	$7.5 \cdot 10^{17}$	$7.4 \cdot 10^{11}$	$5.2 \cdot 10^5$
>1keV	$8.4 \cdot 10^{17}$	$9.2 \cdot 10^8$	640
>2keV	$4.6 \cdot 10^{12}$	$4.8 \cdot 10^6$	3

Table 6. SR backgrounds (from 1 beam) for Variant 2.

Conclusions

SR Backgrounds in the C-Tau interaction region in absence of masks:

1) The maximal area density of SR power on the vacuum chamber wall is $1.4 \text{ BT}/\text{cm}^2$ (from the magnet BV2).

2) The maximal area density of SR power incident on the edge of the ES lower electrodes is $5 \cdot 10^{-3} \text{ BT}/\text{cm}^2$ if the gap width between them is equal to 1cm.

3) When passing the quadrupoles Q4 the beams deposit

0.8 BT or $6.4 \cdot 10^{16} \text{ phot./s}$ (both beams) on the beampipe surface. The energy spectrum of this radiation is much softer than this obtained in design of B-factory /4/ - there are practically no photons with energies of the K lines of Cu (8 KeV) causing induce fluorescence in the beampipe Cu coating. However masking of the direct SR is necessary because of the high dose deposited on the first Si layer.

The both 1-st and 2-nd variants of masking diminish the power incident on the beampipe to $\sim 10^{-5} \text{ W}$ and the photons to $\sim 2 \cdot 10^{12} \text{ phot./s}$. The total number of photons/s entering the detector volume is $\approx 10^6 \text{ phot./s}$, of them $1.3 \cdot 10^3$ have energy $> 1 \text{ keV}$ and ~ 10 have energy $> 2 \text{ keV}$.

According to the results obtained in /3/,/4/ the occupancy of the central tracing chambers and the vertex detectors in such levels of backgrounds is negligible.

REFERENCES

1. V.S.Alexandrov, V.K.Antropov et al., JINR Tau-Charm Factory Design Considerations, - Proceedings of the Workshop on JINR C-tau Factory, Dubna, 29-31 May, 1991, p.225.
2. E.A.Perelstein, V.S.Alexandrov, V.K.Antropov et al., - JINR Tau-Charm Factory Study, XI Intern. Conference on High Energy Accelerators, Hamburg, Germany, July 20-24, 1992.
3. "An Asymmetric B Factory based on PEP", SLAC-372, 1991, p.111.
4. "CESR-B Conceptual Design", CLNS 91-1050, Cornell Univ., pp.4-8.
5. P.Roudeau, Collimators and Masks Against Synchrotron Radiation Backgrounds in a LEP Experimental Area, LEP Note 487, 1984.
6. C.Geyer, K.Balewsky et al., Synchrotron Radiation Calculations and Collimator Design of an Asymmetric B-Factory, DESI Internal Report.

Received by Publishing Department
on March 4, 1993.